SENCKENBERG

ORIGINAL PAPER

Changes in macrofaunal groups before, during and after the Cenomanian–Turonian biotic crisis in north Eastern Desert, Egypt

Shahin Abd-Elhameed[1] · Yasser Salama[2] · Abdelaziz Mahmoud[1]

Abstract

The stratigraphic distribution of the different faunal groups of the upper Cenomanian–lower Turonian deposits in the north Eastern Desert, Egypt, is investigated. Variations in species richness, faunal diversity, extinction and origination rates before, during, and after the globally known Oceanic Anoxic Event (OAE) 2 are documented. The OAE2 interval is constrained by the first occurrence of the marker ammonite species *Vascoceras cauvini* and the last occurrence of *Vascoceras proprium*, along with the positive $\delta^{13}C$ excursions, previously identified from the Wadi El-Burga section. A prominent decline in species richness and diversity, high extinction rates, and low origination rates of the recorded macrofaunal elements are reported during the OAE2 interval. Such faunal bottleneck was attributed to the prevailing major palaeoclimatic and palaeoenvironmental perturbations during that time. Besides oceanic anoxia, changes in sea water palaeotemperature and sea level are discussed. It can be concluded that oceanic anoxia, warming, and /or transgressive episodes were the major driving mechanisms of the faunal crisis reported in the present work.

Introduction

The mid–Cretaceous (Aptian–Turonian) greenhouse conditions reached their peak during the late Cenomanian–early Turonian times (Norris et al. 2002; Forster et al. 2007), with significant warming, high atmospheric carbon dioxide concentration, and major sea–level rise, characterising the prominent Oceanic Anoxic Event 2 (OAE2; Schlanger and Jenkyns 1976; Haq et al. 1987; Harries and Little 1999; Takashima et al. 2006, 2009; Pearce et al. 2009; Jenkyns 2010; Barclay et al. 2010; Ruban et al. 2011; Pogge von Strandmann et al. 2013; Ruban 2013). The OAE2 is usually identified by the deposition of black organic–rich shales and a significant positive $\delta^{13}C$ excursion (Arthur et al. 1988; Tsikos et al. 2004; Mort et al. 2008; Nagm et al. 2014).

Palaeobiologically, OAE2 witnessed the 10th largest extinction event during the Phanerozoic (Raup and Sepkoski 1984; Bambach 2006), characterised by a worldwide drop in faunal diversity (Elder 1989; Kaiho 1994; Leckie et al. 2002; Bambach et al. 2004; Gale et al. 2005; Takashima et al. 2006; Keller et al. 2008; Monnet 2009; Gebhardt et al. 2010; Ruban et al. 2011; Orabi et al. 2012; Ruban 2013; Nagm 2015; Nagm et al. 2017; Li et al. 2017; Owens et al. 2018; Freymueller et al. 2019; Keller et al. 2021). Bambach (2006) estimated that 25% of the marine genera and 33–53% of species went extinct, approximately two and a half times the background-extinction for genera.

In Egypt, the OAE2 was reported based on the positive $\delta^{13}C$ excursion, rather than the presence of organic-rich shales (El-Sabbagh et al. 2011; Nagm et al. 2014, 2021). Despite the extensive literature on the faunal content of the upper Cenomanian–lower Turonian deposits in north Eastern Desert (Kassab and Ismael 1996; Bauer et al. 2001; Hewaidy et al. 2003; Abdel-Gawad et al. 2007; Boukhary et al. 2009; El-Qot et al. 2009; Shahin and El-Baz 2010; Nagm et al. 2010a; Ayoub-Hannaa and Fürsich 2011; El-Sabbagh et al. 2011; Nagm and Wilmsen 2012; Ayoub-Hannaa et al. 2014; Nagm 2015; Boukhary et al. 2017; Nagm 2019), these studies were mainly focused on the taxonomy of the faunal groups and biostratigraphic subdivision of the studied intervals, except for the work of Nagm et al. (2021). Nagm et al. (2021) provided only a general view

✉ Shahin Abd-Elhameed
shahinashraf2014@gmail.com

1 Department of Geology, Faculty of Science, Helwan University, Helwan, Cairo 11731, Egypt

2 Department of Geology, Faculty of Science, Beni-Suef University, Beni-Suef, Egypt

of the faunal change across the OAE2 interval, without any detailed quantitative analysis of the faunal diversity change, extinction, and origination rates.

Therefore, the objectives of the present work are (1) to investigate the stratigraphic distribution of the different faunal groups (cephalopods, bivalves, gastropods, and echinoids) of the well-exposed upper Cenomanian–lower Turonian successions in the north Eastern Desert, Egypt; (2) to illustrate the previously-reported ammonite biozonations along with the defining OAE2 positive δ^{13}C excursion, using the previous δ^{13}C data of Nagm et al. (2014) at Wadi El-Burga area; (3) and to estimate the diversity change, extinction, and origination rates of these faunal groups as a result of the OAE2, using a quantitative occurrence-based approach.

Geological setting

During Late Cretaceous times, Egypt was located at the southern margin of the Neotethys Ocean (Fig. 1a), where a major marine transgression inundated extensive parts of northern Egypt to a palaeolatitude of 23° N in the late Cenomanian. Consequently, shallow marine conditions were developed, and the lower Upper Cretaceous marine deposits formed extensive exposures (Philip and Floquet 2000; Nagm et al. 2010a, b; Wilmsen and Nagm 2012, 2013; Khalifa et al. 2014).

The measured sections are located at Askhar El-Bahari and Umm Khayshar areas, at the Northern and Southern Galala Plateaus, north Eastern Desert, Egypt (Fig. 1b), where the marine Cenomanian–Turonian deposits are well-exposed. These deposits are represented by the mixed siliciclastic-carbonate Galala and Maghra El-Hadida formations (Nagm et al. 2010a; Wilmsen and Nagm 2012, 2013; Nagm 2015).

The studied sections start with the Lower Cretaceous Malha Formation, consisting of non-marine, brown, unfossiliferous sandstones (Figs. 2, 3). The middle–upper Cenomanian Galala Formation unconformably overlies Malha Formation, consisting of shallow-marine, open lagoonal deposits (Wilmsen and Nagm 2012). The lower part is made up of sandstones, mudstones, shales, and marls in the lower part, while the upper part consists of marl-shale-marly limestone intercalations at Umm Khayshar, and limestones and marly limestones at Askhar El-Bahari area, with calcareous algae as well as chondrodontid, rudistid and oyster bivalves (Figs. 2, 3). In addition, the Galala Formation yields a diverse assemblage of oysters, rudists, gastropods, echinoids, and cephalopods. The Galala Formation was deposited in a fully marine lagoonal environment developing in response to a latest middle to early late Cenomanian transgression. The rich suspension and deposit-feeding macrobenthos of the Galala Formation indicate meso- to eutrophic conditions (Wilmsen and Nagm 2012).

A major sedimentary unconformity separates the Galala Formation from the overlying upper Cenomanian–Turonian

Maghra El-Hadida Formation, corresponding to the global mid–late Cenomanian SB Ce5 (Wilmsen and Nagm 2012, 2013). This sequence boundary is characterised by abrupt facies change from the highstand shaley facies and deep subtidal bioclastic floatstone facies of the Galala Formation at Umm Khayshar and Askhar El-Bahari areas, respectively, to the intertidal sandstone facies of the Maghra El-Hadida Formation (Figs. 2, 3). Only the lower part of the Maghra El-Hadida Formation is investigated in the present study, dominated by open-marine carbonate rocks (Figs. 2, 3; Wilmsen and Nagm 2012). It is made up of brownish yellow, fine-grained, calcareous sandstones, followed by highly fossiliferous, fine-grained marly and dolomitic limestones, with diverse ammonoid content of late Cenomanian and early Turonian age (Figs. 2, 3). The Maghra El-Hadida Formation suggests deposition on a homoclinal carbonate ramp with sub-environments ranging from deep-subtidal basin to intertidal back-ramp (Wilmsen and Nagm 2012).

Based on the presence of upper Cenomanian cephalopods in the upper part of the Galala Formation and the lower part of Maghra El-Hadida Formation, the boundary between the two formations lies below the Cenomanian–Turonian boundary, unlike that has been reported in the previous studies (e.g. Hewaidy et al. 2003).

Materials and methods

Two complete stratigraphic sections across the upper Cenomanian–lower Turonian successions at the Northern and Southern Galala Plateaus, north Eastern Desert, Egypt, were measured and investigated (Askhar El-Bahari section: 29° 03′ 04″ N and 32° 01′ 09″ E and Umm Khayshar section: 28° 51′ 54″ N and 32° 9′ 50″ E; Fig. 1b). Fossils were gathered bed-by-bed from the highly fossiliferous intervals and identified to the species level (Online Resources. 1, 2). The stratigraphic ranges of the identified macrofaunal species were carefully traced (Figs. 2, 3). The ammonites were investigated and their stratigraphic ranges were used for biostratigraphic subdivision of the studied interval.

The high-resolution δ^{13}C excursions (OAE2), generated from the Wadi El-Burga section (Nagm et al. 2014), about 40 km to the south of the study area, were incorporated in the present study using the age-defining ammonite biozones (Fig. 4). A sample-species occurrence matrix of the macrofossils was generated for further quantitative analyses (Online Resource. 3). The diversity is calculated for each faunal group, expressed by the species richness (the number of species, with low species richness =<5 species, moderate =5-15 species, and high >15 species) and Shannon-Wiener diversity index (*H*; Shannon 1948) for each interval. The diversity changes of the different faunal groups across the Cenomanian–Turonian boundary were documented in order to identify the different bioevents.
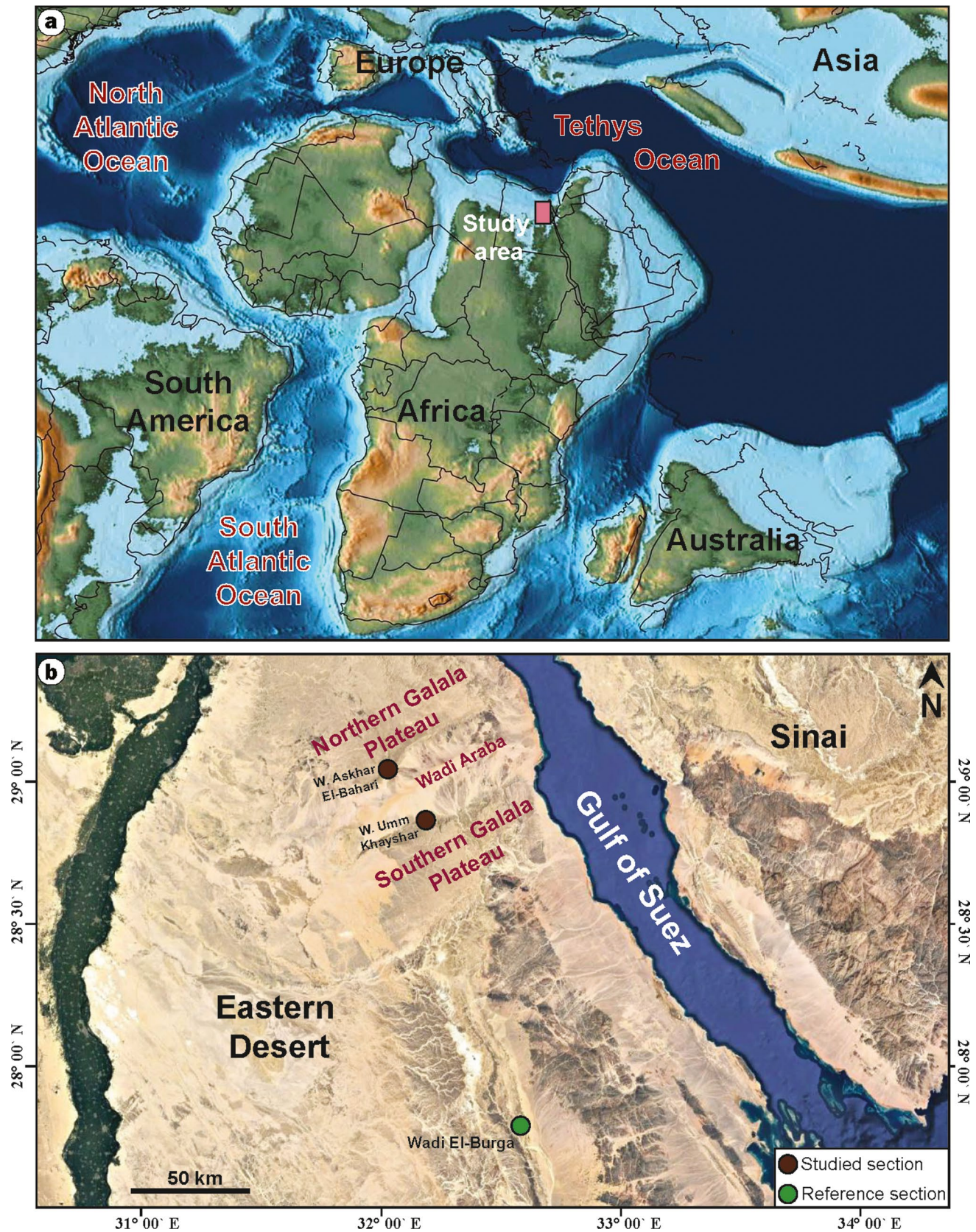
Fig. 1. **a** Late Cenomanian palaeogeographic map, showing the position of the study area (after Scotese 2014). **b** Location of the study area, with indication for the studied and reference sections (Google Earth, earth.google.com/web/)
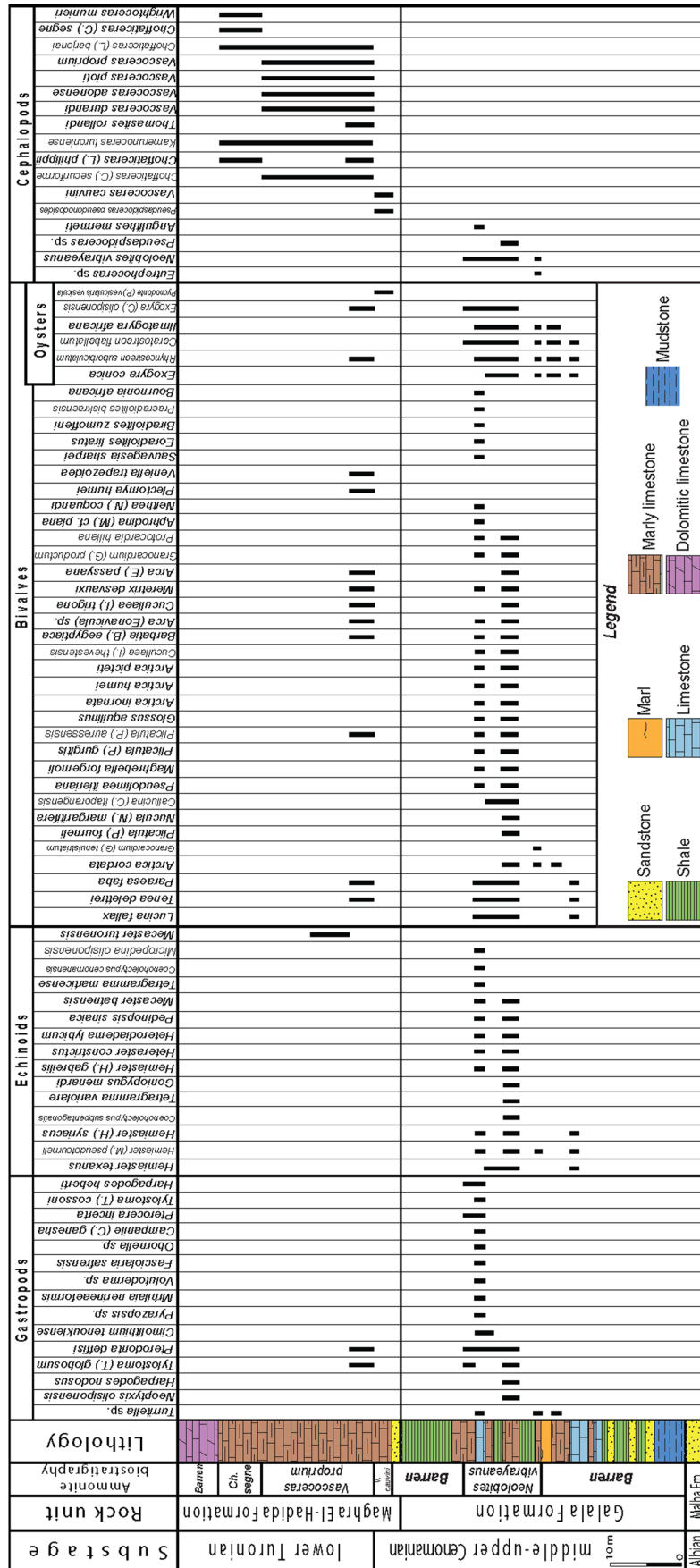
Fig. 2 The stratigraphic section at Umm Khayshar, Southern Galala Plateau, Eastern Desert, Egypt, showing biostratigraphic subdivisions, and range chart of various macroinvertebrates
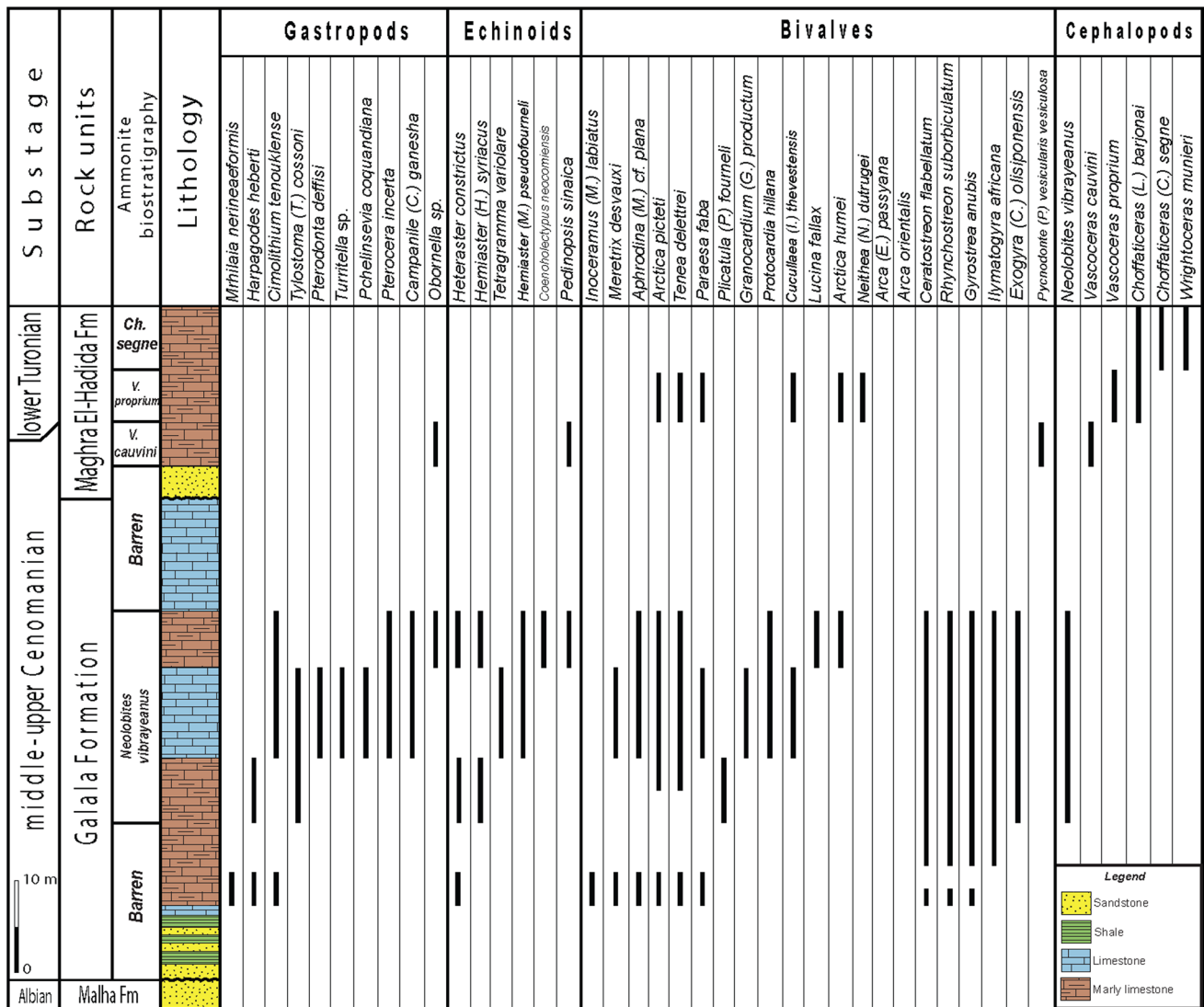
Fig. 3. The stratigraphic section at Askhar El-Bahari, Northern Galala Plateau, Eastern Desert, Egypt, showing biostratigraphic subdivisions, and range chart of various macroinvertebrates

The extinction and origination rates are defined following Kurihara (2012), where the Extinction rate = (number of species absent in an interval) / (total number of species in the preceding interval) × 100%, and the Origination rate = (number of species present in an interval and not present in the preceding one) / (total number of species present in the former interval) × 100%. All material is hosted in the Geological Museum, Helwan University, Cairo, Egypt.

Results

Ammonite biostratigraphy

The studied strata of the north Eastern Desert contain rich ammonite fauna, including the main index taxa of the upper Cenomanian–lower Turonian transition, allowing a high-resolution biostratigraphic subdivision for this time interval. Based on the stratigraphic distribution of the identified ammonite species in the studied sections (Figs. 2, 3), two upper Cenomanian ammonite zones (*Neolobites vibrayeanus* Zone and *Vascoceras cauvini* Zone) and two lower Turonian ammonite zones (*Vascoceras proprium* Zone and *Choffaticeras segne* Zone) have been differentiated.

Neolobites vibrayeanus Zone

The upper Cenomanian *Neolobites vibrayeanus* Zone, which spans the upper part of the Galala Formation in the studied sections, is defined by the total range of *Neolobites vibrayeanus* (Orbigny; Figs. 2, 3). The *Neolobites vibrayeanus*
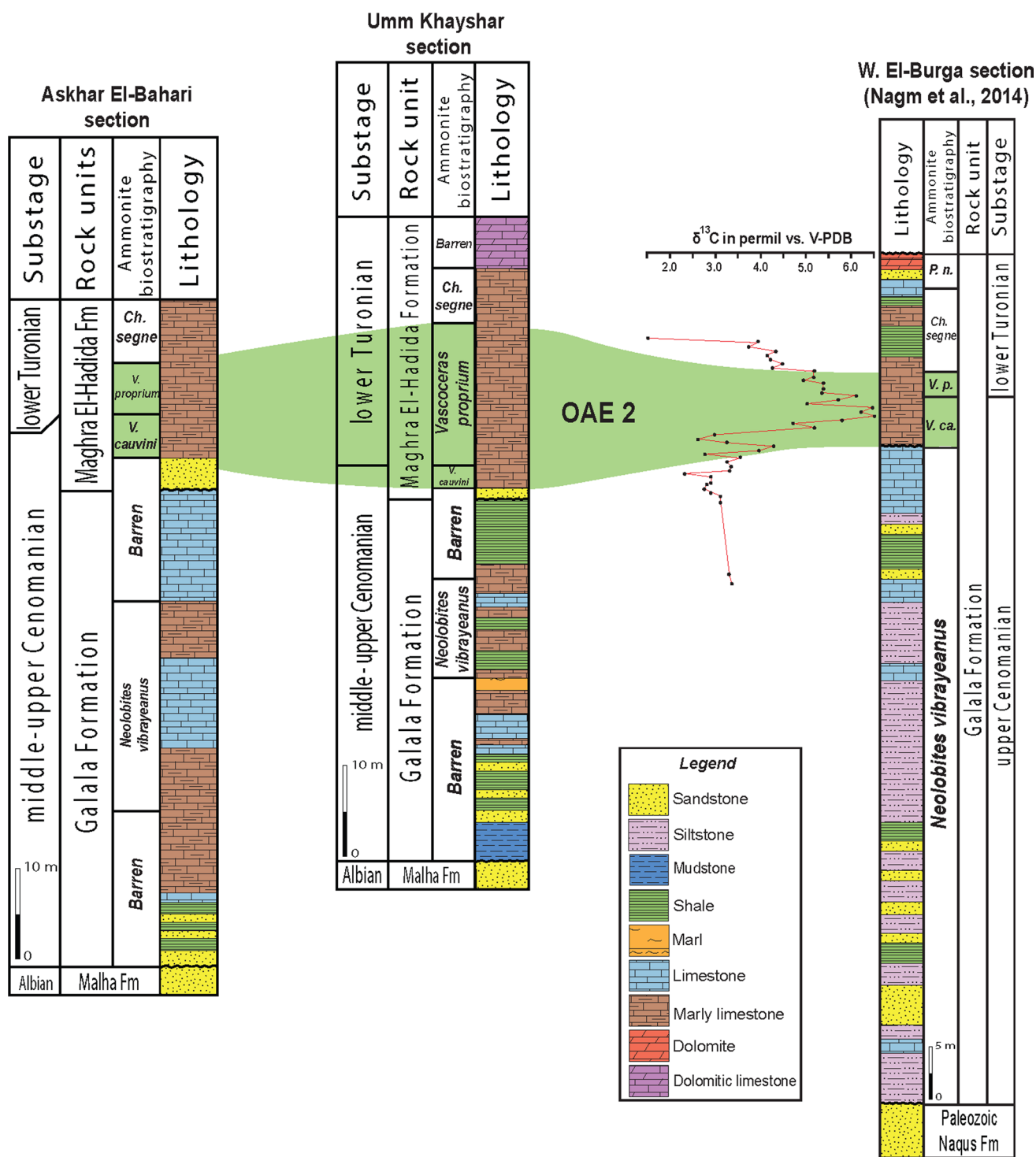
Fig. 4. The stratigraphic section at Umm Khayshar and Askhar El-Bahari, showing the recognised ammonite biozones, and a correlation with the Wadi El-Burga section (Nagm et al. 2014)

Zone overlies the barren middle Cenomanian strata and underlies the barren upper Cenomanian strata that correspond to the upper part of the *Neolobites vibrayeanus* Zone and the *Metoicoceras geslinianum* Zone, recognised by

Nagm et al. (2010a, b) in the Wadi Ghonima section. The zonal marker is associated with a rich macrofaunal content, including the cephalopods *Eutrephoceras* sp., *Pseudaspidoceras* sp., and *Angulithes mermeti* (Coquand); the bivalves

Exogyra (*Costagyra*) *olisiponensis* (Sharpe), *Ceratostreon flabellatum* (Goldfuss), *Rhynchostreon suborbiculatum* (Lamarck), *Ilymatogyra africana* (Lamarck), *Exogyra conica* (Sowerby), *Sauvagesia sharpei* (Bayle), *Eoradiolites liratus* (Conrad), and *Biradiolites zumoffeni* (Douvillé); the gastropods *Pterodonta deffisi* Thomas and Péron, *Tylostoma* (*Tylostoma*) *cossoni* Thomas and Péron, *Tylostoma* (*Tylostoma*) *globosum* Sharpe, *Pterocera incerta* d'Orbigny, *Harpagodes heberti* (Thomas and Péron), and *Harpagodes nodosus* (Sowerby); and the echinoids *Hemiaster* (*Hemiaster*) *syriacus* (Conrad), *Hemiaster* (*Hemiaster*) *gabreilis* Péron and Gauthier, *Hemiaster* (*Mecaster*) *pseudofourneli* Péron and Gauthier, *Heteraster constrictus* (Fourtau), and *Heterodiadema lybicum* (Agassiz and Desor) (Figs. 2, 3).

The *Neolobites vibrayeanus* Zone has been recorded from many areas along the southern and western Tethyan margins, e.g. Tunisia (Abdallah et al. 2000), Algeria (Benyoucef et al. 2019), Morocco (Meister and Rhalmi 2002), Negev (Lewy et al. 1984), Jordan (Aly et al. 2008; Nagm et al. 2017), and Spain (Barroso-Barcenilla and Goy 2007), as well as from the study area (Nagm et al. 2010a, b). It is correlated with the upper Cenomanian *Calycoceras guerangeri* Zone in Europe (Meister and Piuz 2013; Nagm et al. 2017).

Vascoceras cauvini Zone

The uppermost Cenomanian *Vascoceras cauvini* Zone, which spans the lower part of Maghra El-Hadida Formation in the studied sections, is defined by the total range of *Vascoceras cauvini* (Chudeau; Figs. 2, 3). The *Vascoceras cauvini* Zone overlies the barren upper Cenomanian strata and underlies the lower Turonian *Vascoceras proprium* Zone, where the first occurrence of the latter species is considered as the Cenomanian–Turonian boundary marker. The zonal species is associated with *Pseudaspidoceras pseudonodosides* (Choffat), the echinoid *Pedinopsis sinaica* (Desor), the gastropod *Obornella* sp., and the oyster *Pycnodonte (Phygraea) vesicularis vesiculosa* (Sowerby). The *Vascoceras cauvini* Zone represents the terminal Cenomanian interval in Egypt (Nagm et al. 2010a, b, 2021), Tunisia (Abdallah et al. 2000), Morocco (Lehmann and Herbig 2009), the Negev (Lewy et al. 1984), and Jordan (Nagm et al. 2017).

Vascoceras propium Zone

The lower Turonian *Vascoceras propium* Zone, which spans the lower part of Maghra El-Hadida Formation in the studied sections, is defined by the total range of *Vascoceras propium* (Reyment; Figs. 2, 3). The *Vascoceras propium* Zone overlies the uppermost Cenomanian *Vascoceras cauvini* Zone and underlies the middle lower Turonian *Choffaticeras segne* Zone. The zonal marker is associated with *Choffaticeras*

(Choffaticeras) securiforme (Eck), *Choffaticeras (Leoniceras) philippii* (Solger), *Kamerunoceras turoniense* (d'Orbigny), *Thomasites rollandi* (Thomas and Péron), *Vascoceras adonense* Choffat, *Vascoceras durandi* (Thomas and Péron), *Vascoceras pioti* (Péron and Fourtau), and *Choffaticeras (Leoniceras) barjonai* (Choffat).

The gastropod and echinoid taxa in this zone include *Pterodonta deffisi* Thomas and Péron, *Tylostoma* (*Tylostoma*) *globosum* Sharpe, and *Mecaster turonensis* (Fourtau). This zone also encompasses a rich bivalve content, represented by *Tenea delettrei* (Coquand), *Paraesa faba* (Sowerby), *Arca* (*Eonavicula*) sp., *Cucullaea* (*Idonearca*) *trigona* (Seguenza), *Meretrix desvauxi* (Coquand), *Barbatia* (*Barbatia*) *aegyptiaca* (Fourtau), *Plectomya humei* (Fourtau), *Arca* (*Eonavicula*) *passyana* d'Orbigny, and *Veniella trapezoidea* (Conrad).

The *Vascoceras proprium* Zone is the basal Turonian ammonite zone in Egypt (Nagm et al. 2010a, b, 2021) and Jordan (Nagm et al. 2017). This zone is correlated to the *Pseudaspidoceras flexuosum* Zone in Tunisia (Meister and Abdallah 2005), and to the *Vascoceras durandi-Pseudaspidoceras flexuosum* Zone in Morocco (Meister and Rhalmi 2002). Based on the occurrence of *Vascoceras durandi* (Thomas and Peron) and *Vascoceras pioti* (Peron and Fourtau), the *Vascoceras proprium* Zone can be correlated to the lower part of the *Watinoceras devonense/ coloradoense* Zone and the *Pseudaspidoceras flexuosum* Zone in North America (Kennedy and Cobban 1991; Meister and Abdallah 2005; Nagm et al. 2010a, b, 2017).

Choffaticeras segne Zone

The middle lower Turonian *Choffaticeras segne* Zone, which spans the middle part of Maghra El-Hadida Formation in the studied sections, is defined by the total range of *Choffaticeras segne* (Solger; Figs. 2, 3). The *Choffaticeras segne* Zone overlies the lower Turonian *Vascoceras propium* Zone and underlies barren middle Turonian strata. The zonal species is associated with *Choffaticeras (Leoniceras) philippii* (Solger), *Kamerunoceras turoniense* (d'Orbigny), *Wrightoceras munieri* (Pervinquière), *Choffaticeras (Leoniceras) barjonai* (Choffat) and *Choffaticeras (Choffaticeras) segne* (Solger).

The *Choffaticeras segne* Zone has been also recorded from the study area (Nagm et al., 2010a, b) and Jordan (Aly et al. 2008; Nagm et al. 2017). It is correlated to the *Thomasites rollandi* Zone in Tunisia (Chancellor et al. 1994), and the *Choffaticeras* (*Choffaticeras*) *quaasi* and *Spathites* (*Ingridella*) *malladae* zones in Spain (Barroso-Barcenilla and Goy 2007). Furthermore, this zone is regarded as equivalent to the upper part of the standard Tethyan ammonite *Watinoceras devonense* Zone (Gradstein et al. 2004; Nagm et al. 2010a, b, 2017).

Faunal characteristics

Before OAE2

The interval preceding the OAE2 is equivalent to the upper Cenomanian *Neolobites vibrayeanus* Zone (Fig. 4). It contains diverse faunas, represented by bivalves, gastropods, echinoids, and cephalopods, with high species richness (73 species) and diversity ($H = 3$; Fig. 5). The bivalves are the most dominant group (53.5%), with high species richness (39 species) and high diversity ($H = 2.5$). Epifaunal bivalves are the most common ecological group (68.5%), dominated by Gryphaeidae (74.8%) and Radiolitidae (4.1%), while infaunal bivalves are less common (17%), dominated by Arcticidae (7.2%), Veneridae (5.2%), and Cucullaeidae (3.3%) (Figs. 6, 7a).

The echinoids and gastropods also constitute significant portions of the recorded fauna (20.5% for each; Fig. 6). They both show high species richness (15 echinoid and 15 gastropod species) and high diversity ($H = 2.2$ and 2.4, respectively). The echinoids are dominated by Hemiasteridae (66.9%) and Toxasteridae (12.6%), whereas the gastropods are dominated by Procerithiidae (23.4%),

Aporrhaidae (19.7%), Tylostomatidae (14.6%), and Strombidae (11.7%) (Fig. 7b, c).

Cephalopods also occur, but with relatively low species richness (4 species) and low diversity ($H = 0.4$; Fig. 5). The Engonoceratidae is the most dominant family (89.5%), and other families include the Nautilidae, Acanthoceratidae, and Cymatoceratidae (5.3%, 2.6%, and 2.6%, respectively; Fig. 8a). This interval shows low infaunal to non-infaunal taxa percentage (25.3%; Fig. 6). It encompasses a diverse fauna with various feeding modes, dominated by suspension-feeding (85.4%) and deposit-feeding taxa (8.7%; Fig. 6).

During OAE2

The extinction rates between the pre-OAE2 and OAE2 intervals show high values; 100% for cephalopods, 93.3% for echinoids, 80% for gastropods, and 64.1% for bivalves (Fig. 5). On the other hand, the origination rates show high values for cephalopods and echinoids (100% and 50%, respectively), and low values for bivalves and gastropods (18.8% and 0%, respectively; Fig. 5).

The interval representing the OAE2 is equivalent to the uppermost Cenomanian *Vascoceras cauvini* Zone and the lower
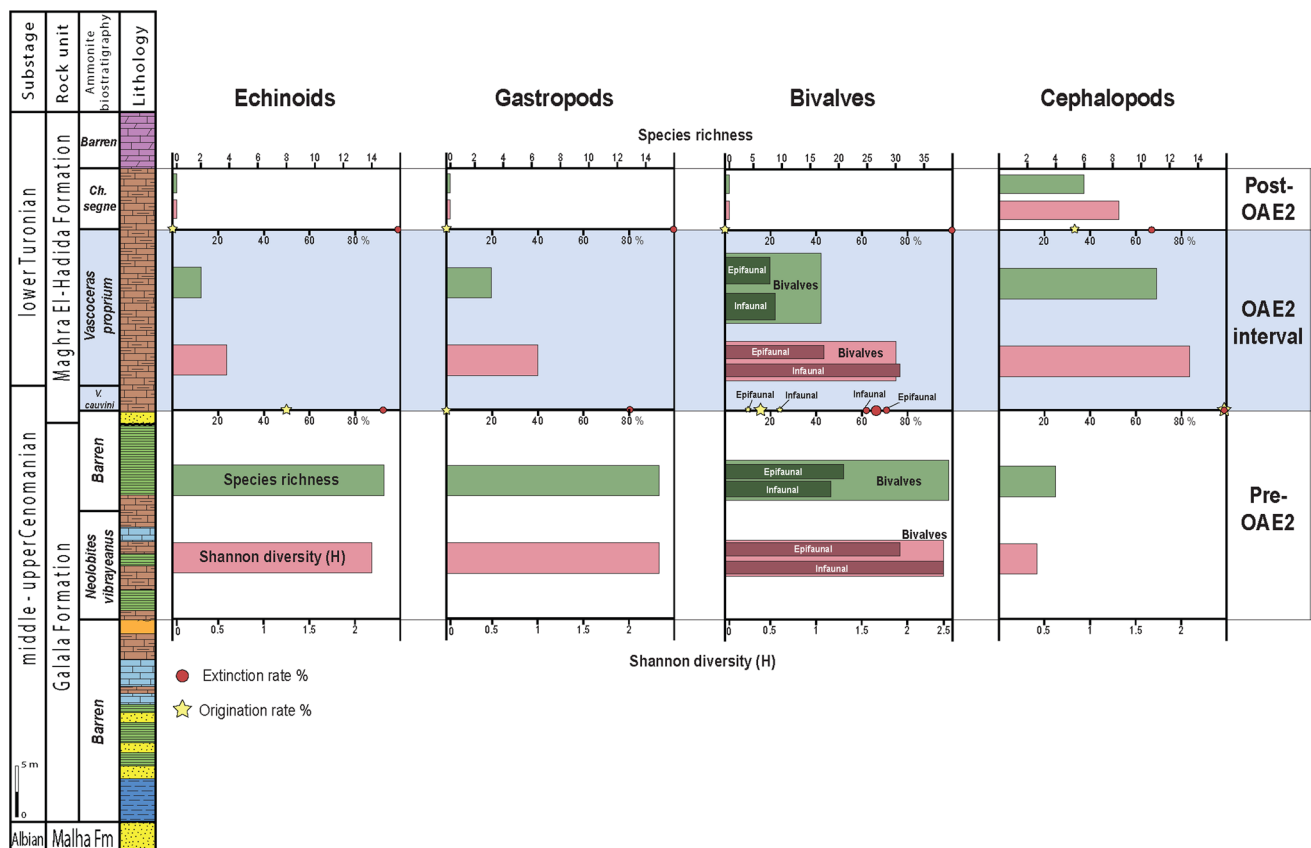

Fig. 5. Representative section for the studied Cenomanian–Turonian successions, showing changes in species richness, diversity, extinction and origination rates before, during, and after the OAE2 interval
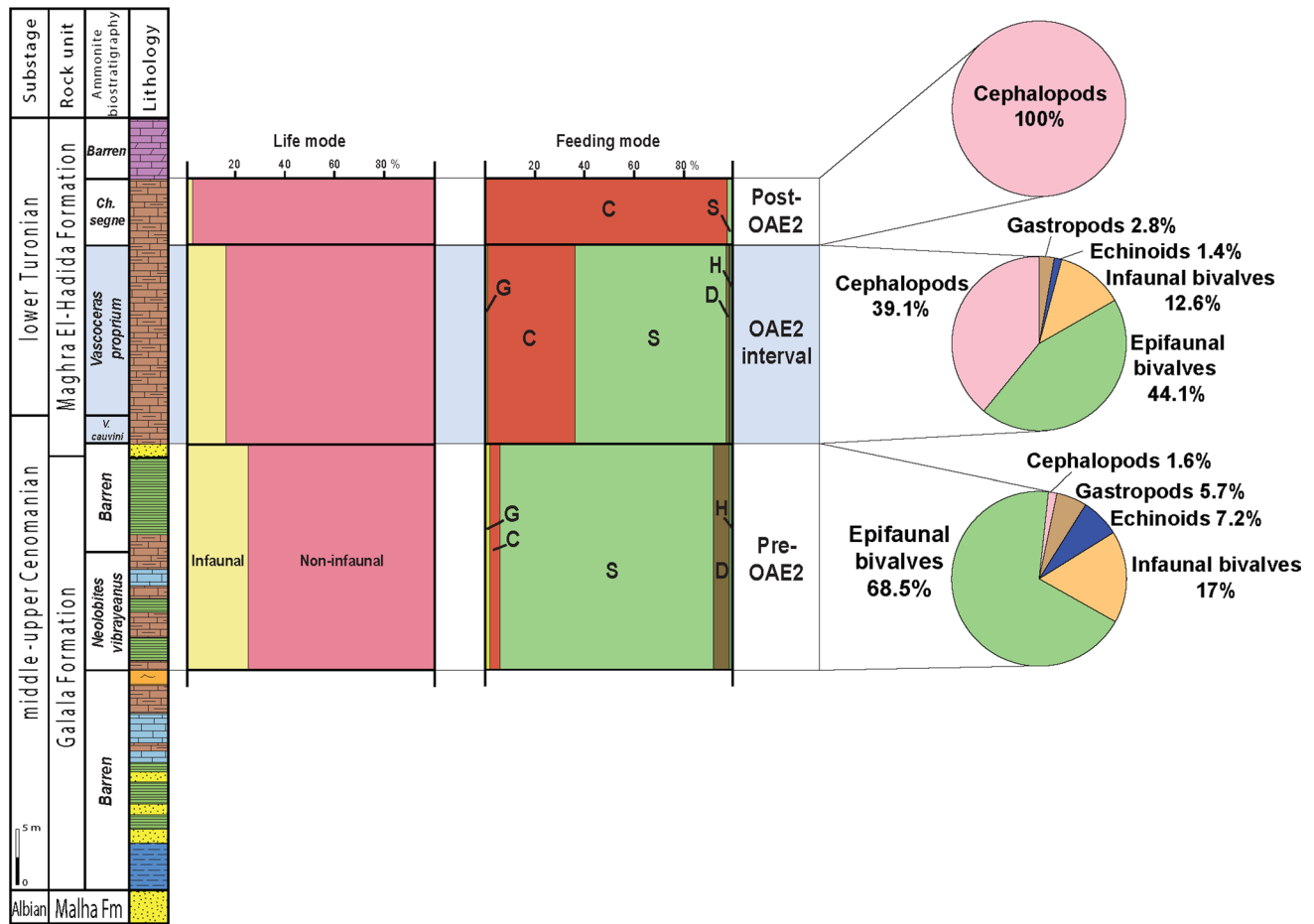
Fig. 6. Representative section for the studied Cenomanian–Turonian successions, showing changes in life mode, feeding strategy, and proportions of faunal groups before, during, and after the OAE2 interval

Turonian *Vascoceras proprium* Zone (Fig. 4). This interval contains diverse faunas, represented by cephalopods, bivalves, gastropods, and echinoids, with relatively moderate species richness (33 species) and high diversity (*H* = 2.74; Fig. 5).

The bivalves and cephalopods are the most dominant groups (56.7% and 39.1%, respectively). This interval shows relatively higher cephalopod species richness (11 species) and higher diversity (*H* = 2.1) than the preceding interval, dominated by pseudotissotiids (46.4%) and vascoceratids (40.5%) (Figs. 6, 8b). The recorded bivalves show moderate species richness (17 species) and diversity (*H* = 1.8), dominated by epifaunal taxa (44.1%) beolonging to the Gryphaeidae (54.9%), Plicatulidae (20.5%), and Arcidae (2.5%) (Fig. 7d). The infaunal bivalve species are less common, representing about 12.6% of the total fauna, and dominated by the Arcticidae (9%) and Veneridae (6.6%) (Fig. 7d).

A few gastropods and echinoids are also recorded, representing about 2.98% and 1.4% of the total fauna, respectively (Fig. 6). The gastropods show low species richness (3 species) and low diversity (*H* = 1; Fig. 5), dominated by the Tylostomatidae (50%), and Pleurotomariidae (33.3%; Fig. 7f). Similarly, the echinoids show low species richness (2 species) and low diversity (*H* = 0.6; Fig. 5), dominated by the Pseudodiadematidae (66.7%; Fig. 7e). This interval shows low infaunal to non-infaunal taxa percentage (18.1%; Fig. 6). The recorded fauna exhibit various feeding modes, dominated by suspension-feeding taxa (60.4%) and carnivores (37.6%; Fig. 6).

After OAE2

The extinction rates between the OAE2 and post-OAE2 intervals also show high values; 100% for echinoids, gastropods, and bivalves, and 63.6% for cephalopods (Fig. 5). On the other hand, the origination rates show low values (33.3% for cephalopods; Fig. 5). The interval succeeding the OAE2 is equivalent to the middle lower Turonian *Choffaticeras segne* Zone (Fig. 4). This interval contains a less diverse fauna, with relatively low species richness (6 species) and low diversity (*H* = 1.3; Fig. 5).
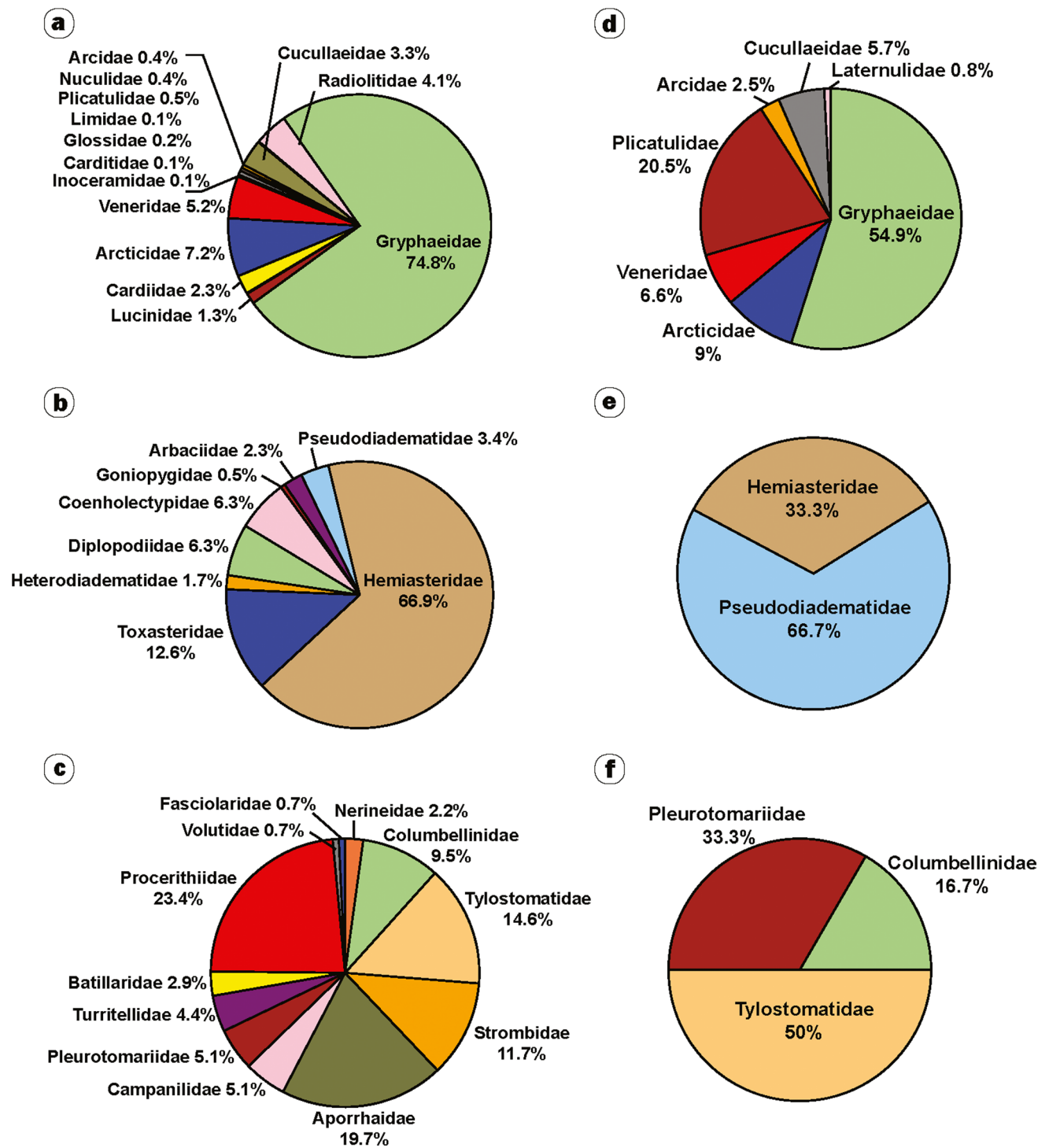
Fig. 7. Individual-based percentages of (**a**) bivalve families before the OAE2 interval. **b** echinoid families before the OAE2 interval. **c** gastropod families before the OAE2 interval. **d** bivalve families during the OAE2 interval. **e** echinoid families during the OAE2 interval. **f** gastropod families during the OAE2 interval
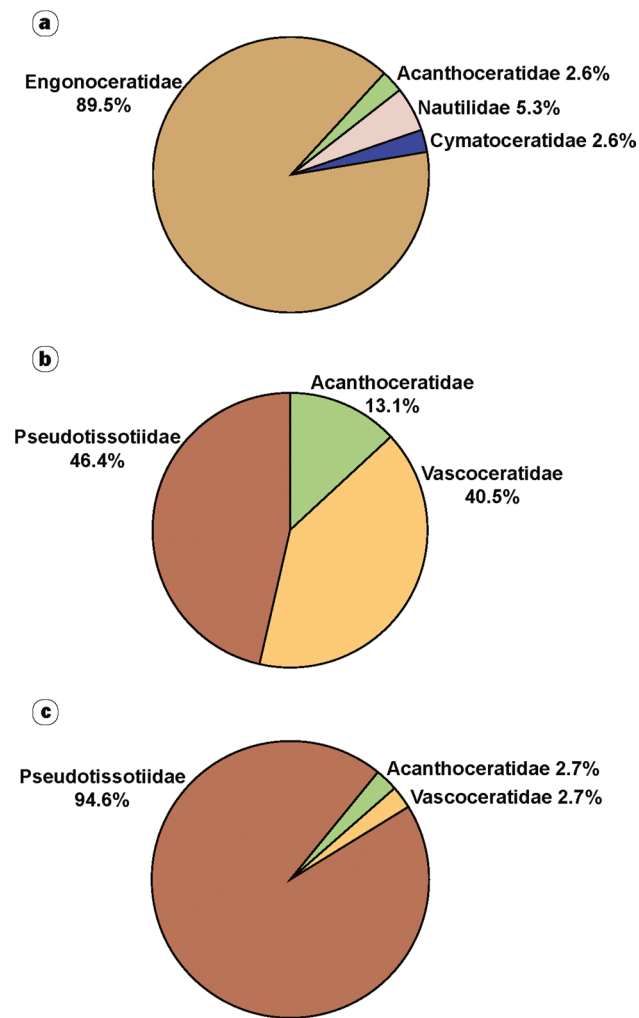
Fig. 8. Individual-based proportions of cephalopod families before (**a**), during (**b**), and after (**c**) the OAE2 interval

The faunal content of this interval is only represented by cephalopods, belonging to the Pseudotissotiidae (94.6%), Acanthoceratidae (2.7%), and Vascoceratidae (2.7%) (Fig. 8c). The recorded fauna in this interval is dominated by carnivore, nektonic species (97.3%; Fig. 6).

Discussion

The Oceanic Anoxic Event 2 is not reflected in the study area by organic-rich shales, but the positive carbon isotope excursion (Nagm et al. 2014; Fig. 4) as well as its negative impact on the faunal diversity can be identified. Such impact on faunal content has been regarded as a global bioevent, being reported in many basins worldwide (Elder 1989; Gale et al. 2000; Keller et al. 2001; Keller and Pardo 2004; Caron et al. 2006; Monnet 2009; Gebhardt et al. 2010; Horne et al. 2011; Kurihara 2012; Ruban 2013; Joo

and Sageman 2014; Nagm 2015; Nagm et al. 2017, 2021; Freymueller et al. 2019).

The stratigraphic ranges of the recorded macroinvertebrates in the Umm Khayshar and Askhar El-Bahari areas, north Eastern Desert, Egypt, illustrate significant faunal changes across the lower and upper boundaries of this mass extinction bioevent (Figs. 2, 3). The lower boundary is characterised by a great drop in the species richness and diversity of echinoids, gastropods, and bivalves across the top of the upper Cenomanian *Neolobites vibrayeanus* Zone. However, cephalopods show rather increase in the species richness and diversity (Fig. 5).

Furthermore, about 79.5% of the total faunal taxa in the interval preceding the OAE2 went extinct (100% of cephalopods, 93.3% of echinoids, 80% of gastropods, and 64.1% of bivalves), and about 87.9% of the faunal taxa recorded in the OAE2 interval originated therein (100% of cephalopods, 50% of echinoids, and 18.8% of bivalves; Fig. 5). A significant drop in the infaunal to non-infaunal taxa (71.5%), and grazer, deposit-feeder, suspension-feeder, and herbivore taxa is documented (Fig. 6).

The upper boundary of this mass extinction bioevent is also characterised by a drop in the species richness and diversity of echinoids, gastropods, bivalves, and cephalopods across the top of the lower Turonian *Vascoceras propium* Zone (Fig. 5). In addition, about 87.9% of the total faunal taxa in the OAE2 interval went extinct (100% of echinoids, gastropods, and bivalves, and 63.6% of cephalopods), and about 33.3% of the cephalopod species recorded in the interval succeeding the OAE2 interval originated (Fig. 5). A nearly complete loss of infaunal taxa, and the dominance of carnivore taxa are observed (Fig. 6), suggesting a new, substantially different ecologic structure. This supports the hypothesis that oceanic anoxic events have most severe negative impact on the infauna than on any other ecological group (Freymueller et al. 2019).

A similar pattern of cephalopod diversity change during OAE2 was documented in Tunisia and Jordan (Monnet 2009; Nagm et al. 2017). Several authors suggested high extinction and origination rates for cephalopods (Elder 1989; Harries and Little 1999; Bambach 2006; Jagt-Yazykova 2011, 2012; Kurihara 2012; Freymueller et al. 2019). The extinction rates of gastropods were unstable through the Late Cretaceous (Ruban 2013). Several studies have reported high extinction level of gastropods, similar to that in the present study, across the Cenomanian–Turonian boundary (Fig. 5; Sohl 1987; Ruban et al. 2011; Nagm 2015).

The bioevent associated with the OAE2 has also resulted in the disappearance of most of the oyster and rudist bivalves, that were considered main features of the late Cenomanian, e.g. *Ilymatogyra africana* (Lamarck), *Ceratostreon flabellatum* (Goldfuss), *Exogyra conica* (Sower-by), *Eoradiolites liratus* (Conrad), *Biradiolites*

zumoffeni (Douvillé), and *Praeradiolites biskraensis* (Coquand) (Figs. 2, 3). This reflects the fact that conditions went too deep for most oysters to thrive following the Cenomanian–Turonian transgression (Abdelhady 2008). A similar case has been reported from worldwide localities (Jones and Nicol 1986; Dhondt et al. 1999; Seeling and Bengston 1999; Abdelhady 2008). The echinoids are well-represented in the late Cenomanian by various families, e.g. Hemiasteridae, Toxasteridae, and Pseudodiadematidae, with only the Hemiasteridae and Pseudodiadematidae surviving into the early Turonian (Figs. 2, 3).

The start of the bioevent coincides with the top of the uppermost Cenomanian *Neolobites vibrayeanus* Zone, about ca. 400 ka before the Cenomanian–Turonian boundary (93.9 Ma; Gradstein et al. 2004, 2012; Nagm 2015). It continued across the Cenomanian–Turonian boundary, and its upper boundary coincides with the top of the lower Turonian *Vascoceras proprium* Zone, about ca. 200 ka after the Cenomanian–Turonian boundary (Nagm 2009, 2015). Consequently, this bioevent lasted for 600 ka in the north Eastern Desert.

The faunal change reported in the present study temporally overlaps well with the OAE2 (Figs. 5, 6), with dramatic changes in species richness and diversity, and various palaeoenvironmental perturbations, e.g. oceanic anoxia, sea water palaeotemperature changes, and sea-level changes (Ruban 2013; Nagm et al. 2017). Oceanic anoxia during the OAE2 were developed in response of the progressive expansion of the oxygen minimum zone through the water column (Schlanger and Jenkyns 1976; Elder 1989; Harries and Little 1999; Kuypers et al. 2004; Monteiro et al. 2012; Pogge von Strandmann et al. 2013; Owens et al. 2018; Freymueller et al. 2019).

Several hypotheses have been introduced concerning the main cause of the OAE2 and the associated mass extinction. Hut et al. (1987), Kauffman (1995), and Kauffman and Hart (1995) hypothesised that a comet shower was the primary cause of that mass extinction. However, Monnet (2009) argued against this hypothesis as the known iridium anomalies were not associated with the faunal diversity decline. The relatively well-founded hypothesis of the cause of the OAE 2 is the emplacement of a large igneous province (LIP; Turgeon and Creaser 2008; Du Vivier et al. 2014; Papadomanolaki et al. 2022). This process resulted in a considerable temperature increase by CO_2 outgassing, enhanced chemical weathering, increased primary production, expansion of the oxygen minimum zone, and formation of black shales (Huber et al. 1995; Bornemann et al. 2005; Monnet 2009; Monteiro et al. 2012; Keller et al. 2021), ultimately triggering the mass extinction associated with OAE 2.

Climatic changes have been associated with OAE2 (Huber et al. 2002; Bornemann et al. 2005; Jenkyns 2010; Pogge von Strandmann et al. 2013; Kuhnt et al. 2017). A global temperature increase was reported during the late Cenomanian, and reached its peak during OAE2, with sea-surface temperatures about 5–10° C higher than today (Jenkyns et al. 1994; Huber et al. 1995; Huber et al. 2002; Weissert and Erba 2004; Jarvis et al. 2006, Forster et al. 2007; Keller et al. 2008; Monnet 2009; Jarvis et al. 2011; Keller et al. 2021). This climate change resulted in an increase of chemical weathering on continents, higher dissolved inorganic matter input into oceans, and therefore higher productivity, giving rise to global dysoxia to anoxia conditions (Monteiro et al. 2012; Lebedel et al. 2015).

OAE2 has been also associated with a major sea-level rise (Arthur et al. 1988; Hernàndez-Romano et al. 1997; Gale et al. 2000; Smith et al. 2001; Parente et al. 2007; Lowery et al. 2014; Nagm et al. 2021). The sea-level raised for 200–250 m above the present level (Haq 2014), globally flooding various platforms, e.g. Yugoslavia (Jenkyns 1991), Mexico (Hernàndez-Romano et al. 1997), Spain (Drzewiecki and Simo 1997), Italy (Parente et al. 2007), Germany (Wilmsen et al. 2010), Oman (Philip et al. 1995), Jordan (Schulze et al. 2005; Nagm et al. 2017), Morocco (Benyoucef and Meister 2015; Lebedel et al. 2013, 2015), and Egypt (El-Sabbagh et al. 2011; Nagm et al. 2021). In addition, vast inland seas developed, including the Western Interior, the Trans-Sahara, and the Trans-India seaways (Gale et al. 2008; Keller et al. 2021).

The transgressive episode characterising Egypt coincides with a prominent reduction in species richness and diversity, and high extinction rates of the recorded faunal groups (Fig. 5). It can be concluded that the faunal bottleneck reported from the north Eastern Desert, Egypt, during the OAE2 interval has been a response to one or combination of several palaeoenvironmental perturbations, e.g. oceanic anoxia, global warming, and/or considerable deepening.

Conclusions

The upper Cenomanian and lower Turonian macrofauna (cephalopods, bivalves, gastropods, and echinoids) from the Umm Khayshar and Askhar El-Bahari sections at the Northern and Southern Galala Plateau, north Eastern Desert, Egypt, are studied. The studied interval is associated with the positive $\delta^{13}C$ excursion, inferred from the previously studied Wadi El-Burga section, characterising the Ocean Anoxic Event 2. A precise biostratigraphic calibration of the interval was conducted using ammonite biozonation.

The interval representing the OAE2 in the study area is equivalent to the uppermost Cenomanian *Vascoceras cauvini* Zone and the lower Turonian *Vascoceras proprium* Zone. Remarkable changes in the macrofaunal distribution patterns are shown against the OAE2, represented by significant losses of most faunal elements, with a prominent decline in species richness and diversity, high extinction rates, and low origination rates. Such OAE2-linked faunal loss is analogous to that of Western Europe, United States, and Jordan.

In the study area, the start of OAE2 is characterised by the extinction of 93.3% of echinoids, 80% of gastropods, 64.1% of bivalves, and 100% of cephalopods. High extinction rates (100% of gastropods, bivalves, and echinoids, and 63.6% of cephalopods) characterise also the end of the OAE2. The dominance of carnivore, nektonic taxa following this biotic crisis indicates that the OAE2 has significantly affected the ecologic structure. The faunal bottleneck during the OAE2 interval reported has been attributed to one or more palaeoenvironmental changes, e.g. oceanic anoxia, warming, and/or a major episode of sea-level rise.

Data availability All data analysed during this study are included in this published article as supplementary material.

Statements and Declarations

Conflict of interest The authors confirm that there is no conflict of interest associated with this publication.

References

Abdallah, H., Sassi, S., Meister, C., & Souissi, R. (2000). Stratigraphie sequentielle et paléogéographie á la limite Cénomanien–Turonien dans la région de Gafsa-Chott area (Tunisie centrale). *Cretaceous Research, 21,* 35–106.

Abdel-Gawad, G. I., El-Qot, G. M., & Mekawy, M. S. (2007). *Macrobiostratigraphy of the Upper Cretaceous succession from southern Galala, Eastern Desert, Egypt. Second international conference of the Tethys* (pp. 329–349). Cairo University.

Abdelhady, A. A. (2008). Cenomanian–Turonian mass extinction of macroinvertebrates in the context of Paleoecology; A case study from North Wadi Qena, Eastern Desert, Egypt. In *Mass Extinction* (pp. 103–127). Berlin, Heidelberg: Springer.

Aly, M.F., Smadi, A., & Abu Azzam, H. (2008). Upper Cenomanian–lower Turonian ammonites of Jordan. *Revue de Paléobiologie, 27 (1),* 43–71.

Arthur, M. A., Dean, W. E., & Pratt, L. M. (1988). Geochemical and climatic effects of increased marine organic carbon burial at the Cenomanian–Turonian boundary. *Nature, 335,* 714–717.

Ayoub-Hannaa, W., & Fürsich, F. T. (2011). Revision of Cenomanian–Turonian (Upper Cretaceous) gastropods from Egypt. *Zitteliana, A. 51,* 115–152.

Ayoub-Hannaa, W., Fürsich, F. T., & El-Qot, G. (2014). Cenomanian–Turonian bivalves from eastern Sinai, Egypt. *Palaeontographica, Abteilung, A. 301 (3-6),* 63–168.

Bambach, R. (2006). Phanerozoic biodiversity mass extinctions. *Annual Review of Earth and Planetary Sciences, 34,* 127–155.

Bambach, R., Knoll, A., & Wang, S. (2004). Origination, extinction, and mass depletions of marine diversity. *Paleobiology, 30,* 522–542.

Barclay, R. S., McElwain, J. C., & Sageman, B. B. (2010). Carbon sequestration activated by a volcanic CO2 pulse during Oceanic Anoxic Event 2. *Nature Geoscience, 3,* 205–208.

Barroso-Barcenilla, F., & Goy, A. (2007). Revision and new data of the ammonite family Pseudotissotiidae in the Iberian Trough, Spain. *Geobios, 40,* 455–487.

Bauer, J., Marzouk, A. M., Steuber, T., & Kuss, J. (2001). Lithostratigraphy and biostratigraphy of the Cenomanian–Santonian strata of Sinai, Egypt. *Cretaceous Research, 22,* 497–526.

Benyoucef, M., & Meister, C. (2015). Lithostratigraphic evolution, facies analysis and depositional environment of the Cenomanian-lower Turonian in the Guir area, Southwestern Algeria. *Cretaceous Research, 53,* 68–88.

Benyoucef, M., Zaoui, D., Adaci, M., Ferré, B., Meister, C., Piuz, A., El-Qot, G. M., Mennad, A., Tchenar, S., & Bensalah, M. (2019). Stratigraphic and sedimentological framework of the Tinrhert Plateau (Cenomanian–Turonian, SE Algeria). *Cretaceous Research, 98,* 95–121.

Bornemann, A., Pross, J., Reichelt, K., Herrle, J. O., Hemleben, C., & Mutterlose, J. (2005). Reconstruction of short-term palaeoceanographic changes during the formation of the late Albian Niveau Breistroffer black shales (Oceanic Anoxic Event 1d, SE France). *Journal of the Geological Society London, 162,* 623–639.

Boukhary, M., Morsi, A., Eissa, R., & Kerdany, M. (2009). Late Cenomanian ostracod faunas from the area south of Ain Sukhna, western side of the Gulf of Suez, Egypt. *Geologia Croatica, 62,* 19–30.

Boukhary, M., Ismail, A. A., & Ghandour, A. A. (2017). *Coxites zubairensis* Smout, 1956: a new record from late Cenomanian of the Southern Galala Plateau, Egypt. *Histrorical Biology, 30,* 531–534.

Caron, M., Dall' Agnolo, S., Accarie, H., Barrera, E., Kauffman, E., Amédro, F., & Robaszynski, F. (2006). High-resolution stratigraphy of the Cenomanian–Turonian boundary interval at Pueblo (USA) and Wadi Bahloul (Tunisia): stable isotope and bioevents correlation. *Geobios, 39,* 171–200.

Chancellor, G. R., Kennedy, W. J., & Hancock, J. M. (1994). Turonian ammonite faunas from central Tunisia. *Special Papers in Palaeontology, 50,* 1–188.

Dhondt, A. V., Malchus, N., Boumaza, L., & Jaillard, E. (1999). Cretaceous oysters from North Africa; origin and distribution. *Bulletin de la Société Géologique de France, 170,* 67–76.

Drzewiecki, P. A., & Simo, J. A. (1997). Carbonate platform drowning and oceanic anoxic events on a mid–Cretaceous carbonate platform, south-central Pyrenees, Spain. *Journal of Sedimentary Research, 67 (4),* 698–714.

Du Vivier, A. D. C., Selby, D., Sageman, B. B., Jarvis, I., Gröcke, D. R., & Voigt, S. (2014). Marine 187Os/188Os isotope stratigraphy

reveals the interaction of volcanism and ocean circulation during Oceanic Anoxic Event 2. *Earth and Planetary Science Letters, 389,* 23–33.

Elder, W. P. (1989). Molluscan extinction patterns across the Cenomanian–Turonian stage boundary in the Western Interior of the United States. *Paleobiology, 15,* 299–320.

El-Qot, G. M., Fürsich, F. T., Abdel-Gawad, G., & Ayoub-Hannaa, W. (2009). Taxonomy and palaeoecology of Cenomanian–Turonian (Upper Cretaceous) echinoids from eastern Sinai, Egypt. *Beringeria, 40,* 55–98.

El-Sabbagh, A., Tantawy, A., Keller, G., Khozyem, H., Spangenberg, J., Adatte, T., & Gertsch, B. (2011). Stratigraphy of the Cenomanian–Turonian oceanic anoxic event OAE2 in shallow shelf sequences of NE Egypt. *Cretaceous Research, 32,* 705–722.

Forster, A., Schouten, S., Moriya, K., Wilson, P. A., & Sinninghe-Damste, J. S. (2007). Tropical warmig and intermittent cooling during the Cenomanian/Turonian oceanic anoxic event 2: sea surface temperature records from the equatorial Atlantic. *Paleoceanography, 22,* PA1219.

Freymueller, N. A., Moore, J. R., & Myers, C. E. (2019). An analysis of the impacts of Cretaceous oceanic anoxic events on global molluscan diversity dynamics. *Paleobiology, 45(2),* 280–295.

Gale, A. S., Smith, A. B., Monks, N. E. A., Young, J. A., Howard, A., Wray, D. S., & Huggett, J. M. (2000). Marine biodiversity through the late Cenomanian–early Turonian: Palaeoceanographic controls and sequence stratigraphic biases. *Journal of the Geological Society, London, 157,* 745–757.

Gale, A. S., Kennedy, W. J., Voigt, S., & Walaszczyk, I. (2005). Stratigraphy of the upper Cenomanian–lower Turonian Chalk succession at Eastbourne, Sussex, UK: ammonites, inoceramid bivalves and stable carbon isotopes. *Cretaceous Research, 26(3),* 460–487.

Gale, A. S., Voigt, S., Sageman, B. B., & Kennedy, W. J. (2008). Eustatic sea-level record for the Cenomanian (Late Cretaceous): Extension to the Western Interior Basin, USA. *Geology, 36,* 859–862.

Gebhardt, H., Friedrich, O., Schenk, B., Fox, L., Hart, M., & Wagreich, M. (2010). Paleoceanographic changes at the northern Tethyan margin during the Cenomanian–Turonian Oceanic Anoxic Event (OAE-2). *Marine Micropaleontology, 77,* 25–45.

Gradstein, F. M., Ogg, J. G., & Smith, A. G. (2004). A Geologic Time Scale 2004 (pp. 1-589). *Cambridge University Press,*

Gradstein, F. M., Ogg, J. G., & Hilgen, F. J. (2012). On the Geologic Time Scale. *Newsletters on Stratigraphy, 45,* 171–188.

Haq, B. U. (2014). Cretaceous eustasy revisited. *Global Planetary Change, 113,* 44–58.

Haq, B.U., Hardenbol, J., & Vail, P. R. (1987). Chronology of fluctuating sea levels since the Triassic. *Science, 235,* 1156–1167.

Harries, P. J., & Little, C. T. S. (1999). The early Toarcian (Early Jurassic) and the Cenomanian–Turonian (Late Cretaceous) mass extinctions: similarities and contrasts. *Palaeogeography, Palaeoclimatology, Palaeoecology, 154,* 39–66.

Hernàndez-Romano, U., Aguilera-Franco, N., Martinez-Medrano, M., & Barcelo-Duarte, J. (1997). Guerrero-Morelos Platform drowning at the Cenomanian–Turonian boundary, Huitziltepec area, Guerrero State, southern Mexico. *Cretaceous Research, 18,* 661–686.

Hewaidy, A. A., Azab, M. M., & Farouk, S. (2003). Ammonite biostratigraphy of the Upper Cretaceous succession in the area west of Wadi Araba, north Eastern Desert, Egypt. *Egyptian Journal of Paleontology, 3,* 331–359.

Horne, D. J., Brandão, S. N., & Slipper, I. J. (2011). The Platycopid Signal deciphered: Responses of ostracod taxa to environmental change during the Cenomanian–Turonian Boundary Event (Late Cretaceous) in SE England. *Palaeogeography Palaeoclimatology Palaeoecology, 308,* 304–312.

Huber, B. T., Hodell, D. A., & Hamilton, C. P. (1995). Middle–late Cretaceous climate of the southern high latitudes: stable isotopic evidence for minimal equator-to-pole thermal gradients. *Geological Society of America Bulletin, 107,* 1164–1191.

Huber, B. T., Norris, R. D., & MacLeod, K. G. (2002). Deep-sea paleotemperature record of extreme warmth during the Cretaceous. *Geology, 30,* 123–126.

Hut, P., Alvarez, W., Elder, W. P., Hansen, T., Kauffman, E. G., Keller, G., Shoemaker, E. M., & Weissman, P. R. (1987). Comet showers as a cause of mass extinctions. *Nature, 329,* 118–126.

Jagt-Yazykova, E. (2011). Paleobiogeographical and paleobiological aspects of mid– and Late Cretaceous ammonite evolution and bio-events in the Russian Pacific. *Scripta Geologica, 143,* 15–121.

Jagt-Yazykova, E. (2012). Ammonite faunal dynamics along across bio-events during the mid– and Late Cretaceous along the Russian Pacific Coast. *Acta Paleontologica Polonica, 57,* 737–748.

Jarvis, I., Gale, A. S., Jenkyns, H. C., & Pearce, M. A. (2006). Secular variation in Late Cretaceous carbon isotopes and sea-level change: Evidence from a new d^{13}C carbonate reference curve for the Cenomanian–Campanian (99.6-70.6 Ma). *Geological Magazine, 143,* 561–608.

Jarvis, I., Lignum, J. S., Gröcke, D. R., Jenkyns, H. C., & Pearce, M. A. (2011). Black shale deposition, atmospheric CO_2 drawdown, and cooling during the Cenomanian–Turonian Oceanic Anoxic Event. *Paleoceanography and Paleoclimatology, 26,* PA3201.

Jenkyns, H. C. (1991). Impact of Cretaceous sea level rise and anoxic events on the Mesozoic carbonate platform of Yugoslavia. *AAPG Bulletin, 75,* 1007–1017.

Jenkyns, H. C. (2010). Geochemisty of oceanic anoxic events. *Geochemisty, Geophysics, Geosystems, 11,* Q03004.

Jenkyns, H. C., Gale, A. S., & Corfield, R. M. (1994). Carbon and oxygen-isotope stratigraphy of the English Chalk and Italian Scaglia and its palaeoclimatic significance. *Geological Magazine, 131,* 1–34.

Jones, D. S., & Nicol, D. (1986). Origination, survivorship, and extinction of rudist taxa. *Journal of Paleontology, 60,* 107–115.

Joo, Y., & Sageman, B. (2014). Cenomanian to Campanian carbon isotope chemostratigraphy from the Western Interior Basin, USA. *Journal of Sedimentary Research, 84,* 529–542.

Kaiho, K. (1994). Planktonic and benthic foraminiferal extinction events during the last 100 m.y. *Palaeogeography, Palaeoclimatology, Palaeoecology, 111,* 45–74.

Kassab, A. S., & Ismael, M. M. (1996). Biostratigraphy of the Upper Cretaceous sequence of the Gebel Musabaa Salama area, southwest Sinai, Egypt. *Arab Gulf Journal of Scientific Research, 14 (1),* 63–78.

Kauffman, E. G. (1995). Global Change Leading to Biodiversity Crisis in a Greenhouse World: The Cenomanian–Turonian (Cretaceous) Mass Extinction, Effects of Global Change on Life. *Panel on Effects of Past Global Change on Life, National Research Council,* 47–71.

Kauffman, E. G., & Hart, M. B. (1995). Cretaceous bio-events. In O.H. Walliser (Ed.), *Global events and Event Stratigraphy in the Phanerozoic: Results of the International Interdisciplinary Co-operation in the IGCP Project 216 (*pp. 285–304*).* Berlin: Springer Verlag.

Keller, G., Han, Q., Adatte, T., & Burns, S. (2001). Palaeoenvironment of the Cenomanian–Turonian transition at Eastbourne, England. *Cretaceous Research, 22,* 391–422.

Keller, G., & Pardo, A. (2004). Age and paleoenvironment of the Cenomanian–Turonian global stratotype section and point at Pueblo, Colorado. *Marine Micropaleontology, 51,* 95–128.

Keller, G., Adatte, A., Berner, Z., Chellai, E.H., & Stueben, D. (2008). Oceanic events and biotic effects of the Cenomanian–Turonian

anoxic event, Tarfaya Basin, Morocco. *Cretaceous Research, 29,* 976–994.

Keller, G., Nagori, M. L., Chaudhary, M., Reddy, A. N., Jaiprakash, B. C., Spangenberg, J. E., Mateo, P., & Adatte, T. (2021). Cenomanian–Turonian sea-level transgression and OAE2 deposition in the Western Narmada Basin, India. *Gondwana Research, 94,* 73–86.

Kennedy, W. J., & Cobban, W. A. (1991). Stratigraphy and interregional correlation of the Cenomanian–Turonian transition in the Western Interior of the United States near Pueblo, Colorado, a potential boundary stratotype for the base of the Turonian Stage. *Newsletter on Stratigraphy, 24,* 1–33.

Khalifa, M. A., Abu El-Ghar, M. S., Helal, S. A., & Hussein, A. W. (2014). Sequence stratigraphy of the Cenomanian Galala formation, north Eastern Desert. *Journal of African Earth Sciences, 89,* 133–148.

Kuhnt, W., Holbourn, A. E., Beil, S., Aquit, M., Tim Krawczyk, M. T., Flögel, S., Chellai, H., & Jabour, H. (2017). Unraveling the onset of cretaceous Oceanic Anoxic event 2 in an extended sediment archive from the Tarfaya-Laayoune Basin, Morocco. *Paleoceanography and Paleoclimatology, 32,* 923–946.

Kurihara, K., Toshimitsu, S., & Hirano, H. (2012). Ammonoid biodiversity changes across the Cenomanian–Turonian boundary in the Yezo Group, Hokkaido, Japan. *Acta Palaeontologica Polonica, 57 (4),* 749–757.

Kuypers, M., Lourens, L., Rijpstra, W., Pancost, R., Nijenhuis, I., & Sinninghe Damsté, J. (2004). Orbital forcing of organic carbon burial in the proto-North Atlantic during ocean anoxic event 2. *Earth and Planetary Science Letters, 228,* 465–482.

Lebedel, V., Lezin, C., Andreu, B., Wallez, M. J., Ettachfini, E. M., & Riquier, L. (2013). Geochemical and palaeoecological record of the Cenomanian–Turonian Anoxic Event in the carbonate platform of the Preafrican Trough, Morocco. *Palaeogeography, Palaeoclimatology, Palaeoecology, 369,* 79–98.

Lebedel, V., Lézin, C., Andreu, B., Ettachfini, E. M., & Grosheny, D. (2015). The upper Cenomanian–lower Turonian of the Preafrican Trough (Morocco): Platform configuration and palaeoenvironmental conditions. *Journal of African Earth Sciences, 106,* 1–16.

Leckie, R., Bralower, T., & Cashman, R. (2002). Oceanic anoxic events and planktonic evolution: biotic response to tectonic forces during the mid–Cretaceous. *Paleoceanography, 17,* 1–29.

Lehmann, J., & Herbig, H. G. (2009). Late Cretaceous ammonites from the Bou Angueur syncline (Middle Atlas, Morocco)-stratigraphic and palaeobiogeographic implications. *Palaeontographica, A. 289,* 45–87.

Lewy, Z., Kennedy, W. J., & Chancellor, G. R. (1984). Co-occurrence of *Metoicoceras geslinianum* (d'Orbigny) and *Vascoceras cauvini* Chudeau (Cretaceous Ammonoidea) in the southern Negev (Israel) and its stratigraphic implications. *Newsletters on Stratigraphy, 13,* 67–76.

Li, X., Montañez, I., Liu, Z., & Ma, L. (2017). Astronomical constraints on global carbon-cycle perturbation during ocean anoxic event 2 (OAE2). *Earth and Planetary Science Letters, 462,* 35–46.

Lowery, C. M., Corbett, M. J., Leckie, R. M., Watkins, D., Romero, A. M., & Pramudito, A. (2014). Foraminiferal and nannofossil paleoecology and paleoceanography of the Cenomanian–Turonian Eagle Ford Shale of southern Texas. *Palaeogeography Palaeclimatology Palaeoecology, 413,* 49–65.

Meister, C., & Abdallah, H. (2005). Précision sur les successions d'ammonites du Cénomanien–Turonien dans la région de Gafsa, Tunisie du centre-sud. *Revue de Paléobiologie, 24,* 111–199.

Meister, C., & Piuz, A. (2013). Late Cenomanian–early Turonian ammonites of the southern Tethys margin from Morocco to Oman: Biostratigraphy, paleobiogeography and morphology. *Cretaceous Research, 44,* 83–103.

Meister, C., & Rhalmi, M. (2002). Quelques ammonites du Cénomanien–Turonien de la région d'Errachidia-Boudnid-Erfoud (partie méridionale du Haut Atlas Central, Maroc). *Revue de Paléobiologie, 21,* 759–779.

Monnet, C. (2009). The Cenomanian–Turonian boundary mass extinction (Late Cretaceous): new insights from ammonoid biodiversity patterns of Europe, Tunisia, and the Western Interior (North America). *Palaeogeography, Palaeoclimatology, Palaeoecology, 282,* 88–104.

Monteiro, F. M., Pancost, R. D., Ridgwell, A., & Donnadieu, Y. (2012). Nutrients as the dominant control on the spread of anoxia and euxinia across the Cenomanian–Turonian oceanic anoxic event (OAE2): model-data comparison. *Paleoceanography, 27,* 1–17.

Mort, H., Adatte, T., Keller, G., Bartels, D., Föllmi, K., Steinmann, P., Berner, Z., & Chellai, E. H. (2008). Organic carbon deposition and phosphorus accumulation during Oceanic Anoxic Event 2 in Tarfaya, Morocco. *Cretaceous Research, 29,* 1008–1023.

Nagm, E. (2009). *Integrated stratigraphy, palaeontology and facies analysis of the Cenomanian–Turonian (Upper Cretaceous) Galala and Maghra el Hadida formations of the western Wadi Araba, Eastern Desert, Egypt* (pp. 1–213). PhD thesis. Würzburg University.

Nagm, E. (2015). Stratigraphic significance of rapid faunal change across the Cenomanian–Turonian boundary in the Eastern Desert, Egypt. *Cretaceous Research, 52,* 9–24.

Nagm, E. (2019). The late Cenomanian maximum flooding *Neolobites* bioevent: a case study from the Cretaceous of northeast Egypt. *Marine and Petroleum Geology, 102,* 740–750.

Nagm, E., & Wilmsen, M. (2012). Late Cenomanian–Turonian (Cretaceous) ammonites from Wadi Qena, central Eastern Desert, Egypt: taxonomy, biostratigraphy and palaeobiogeographic implications. *Acta Geologica Polonica, 62 (1),* 63–89.

Nagm, E., Wilmsen, M., Aly, M. F., & Hewaidy, A. (2010a). Biostratigraphy of the upper Cenomanian–Turonian (lower Upper Cretaceous) successions of the western Wadi Araba, Eastern Desert, Egypt. *Newsletters on Stratigraphy, 44,* 17–35.

Nagm, E., Wilmsen, M., Aly, M. F., & Hewaidy, A. (2010b). Cenomanian–Turonian (Cretaceous) ammonoids from the western Wadi Araba area, Eastern Desert, Egypt. *Cretaceous Research, 31,* 473–499.

Nagm, E., El-Qot, G., & Wilmsen, M. (2014). Stable-isotope stratigraphy of the Cenomanian–Turonian (upper Cretaceous) boundary event (CTBE) in Wadi Qena, Eastern Desert, Egypt. *Journal of African Earth Sciences, 100,* 524–531.

Nagm, E., Farouk, S., & Ahmad, F. (2017). The Cenomanian–Turonian boundary in Jordan: ammonite biostratigraphy and faunal turnover. *Geobios, 50,* 37–47.

Nagm, E., Jain, S., Mahfouz, K., El-Sabbagh, A., & Shama, A. A. (2021). Biotic response to the latest Cenomanian drowning and OAE2: A case study from the Eastern Desert of Egypt. *Proceedings of the Geologists' Association, 132(1),* 70–92.

Norris, R. D., Bice, K. L., Magno, E. A., & Wilson, P.A. (2002). Jiggling the tropical thermostat in the Cretaceous hothouse. *Geology, 30,* 299–302.

Orabi, O. H., Osman, R. A., El-Qot, G. M., & Afify, A. M. (2012). Biostratigraphy and stepwise extinctions of the larger foraminifera during Cenomanian (Upper Cretaceous) of Gebel Um Horeiba (Mittla Pass), west-central Sinai, Egypt. *Revue de Paléobiologie, Genève, 31(2),* 303–312.

Owens, J., Lyons, T., & Lowery, C. (2018). Quantifying the missing sink for global organic carbon burial during a Cretaceous oceanic anoxic event. *Earth and Planetary Science Letters, 499,* 83–94.

Papadomanolaki, N. M., van Helmond, N. A. G. M., Pälike, H. Sluijs, A., & Slomp, C. P. (2022). Quantifying volcanism and organic carbon burial across Oceanic Anoxic Event 2. *Geology, 50,* 511–515.

Parente, M., Frijia, G., & Di Lucia, M. (2007). Carbon-isotope stratigraphy of Cenomanian–Turonian platform carbonates from the southern Appennines (Italy): a chemostratigraphic approach to the problem of correlation between shallow-water and deep-water successions. *Journal of the Geological Society, London, 164,* 609–620.

Pearce, M. A., Jarvis, I., & Tocher, B. A. (2009). The Cenomanian–Turonian boundary event, OAE2 and palaeoenvironmental change in epicontinental seas: New insights from the dinocyst and geochemical records. *Palaeogeography, Palaeoclimatology, Palaeoecology, 280,* 207–234.

Philip, J., & Floquet, M. (2000). Late Cenomanian (94.7-93.5). In J. Dercourt, M. Gaetani, B. Vrielynck, E. Barrier, B. Biju-Duval, M. F. Brunet, J. P.Cadet, S. Crasquin, M. Sandulescu (Eds.), *Atlas Peri-Tethys* (pp. 129–136). Palaeogeographical Maps. Paris: CCGM/CGMW.

Philip, J., Borgomano, J., & Al-Maskiry, S. (1995). Cenomanian–early Turonian carbonate platform of Northern Oman: stratigraphy and palaeoenvironments. *Palaeogeography, Palaeoclimatology, Palaeoecology, 119,* 77–92.

Pogge von Strandmann, P. A. E., Jenkyns, H. C., & Woodfine, R. G. (2013). Lithium isotope evidence for enhanced weathering during Oceanic Anoxic Event 2. *Nature Geoscience, 6,* 668–672.

Raup, D. M., & Sepkoski, J. J. (1984). Periodicity of extinctions in the geologic past. *Proceedings of the National Academy of Sciences of the United States of America, 81,* 801–805.

Ruban, D. A. (2013). Were Late Cretaceous extinctions of gastropods selective by generic longevity? *Geoscience Frontiers, 4*(1), 87–93.

Ruban, D. A., Forster, A., & Desmares, D. (2011). Late Cretaceous marine biodiversity dynamics in the Eastern Caucasus, northern Neo-Tethys Ocean: regional imprints of global events. *Geoloski anali Balkanskoga poluostrva, 72,* 29–46.

Schlanger, S. O., & Jenkyns, H. C. (1976). Cretaceous oceanic anoxic events: Causes and consequences. Netherlands. *Journal of Geosciences, 55,* 179–184.

Schulze, F., Kuss, J., & Marzouk, A. (2005). Platform configuration, microfacies and cyclicities of the upper Albian to Turonian of west-central Jordan. *Facies, 50,* 505–527.

Scotese, C. R. (2014). *Atlas of Late Cretaceous Maps, PALEOMAP Atlas for ArcGIS, volume 2.* The Cretaceous, Maps 16–22, Mollweide Projection, PALEOMAP Project, Evanston, IL.

Seeling, J., & Bengston, P. (1999). Cenomanian oysters from the Sergipe Basin, Brazil. *Cretaceous Research, 20,* 747–765.

Shahin, A. M., & El-Baz, S. M. (2010). Larger benthic foraminifera from the Cenomanian carbonate platform in southwestern Sinai, Egypt. *Egyptian Journal of Paleontology, 10,* 145–178.

Shannon, C. E. (1948). A mathematical theory of communication. *The Bell System Technical Journal, 27,* 623–656.

Smith, A. B., Gale, A. S., & Monks, N. E. A. (2001). Sea-level change and rock-record bias in the Cretaceous: a problem for extinction and biodiversity studies. *Paleobiology, 27 (2),* 241–253.

Sohl, N. F. (1987). Cretaceous gastropods-contrasts between Tethys and Temperate provinces. *Journal of Paleontology, 61,* 1085–1111.

Takashima, R., Nishi, H., Huber, B. T., & Leckie, R. M. (2006). Greenhouse World and the Mesozoic Ocean. *Oceanography, 19 (4),* 82–92.

Takashima, R., Nishi, H., Hayashi, K., Okada, H., Kawahata, H., Yamanaka, T., Fernando, A. G., & Mampuku, M. (2009). Litho-, bio-and chemostratigraphy across the Cenomanian/Turonian boundary (OAE 2) in the Vocontian Basin of southeastern France. *Palaeogeography, Palaeoclimatology, Palaeoecology, 273(1–2),* 61–74.

Tsikos, H., Jenkyns, H. C., Walsworth-Bell, B., Petrizzo, M. R., Erba, E., Premoli-Silva, I., Forster, A., Kolonic, S., Wagner, T., & Sinninghe Damste, J. S. (2004). Carbon isotope stratigraphy recorded by the Cenomanian/Turonian Oceanic Anoxic Event: Correlation and implications based on three key-localities. *Journal of the Geological Society London, 161,* 711–719.

Turgeon, S. C., & Creaser, R. A. (2008). Cretaceous oceanic anoxic event 2 triggered by a massive magmatic episode. *Nature, 454,* 323–326.

Weissert, H., & Erba, E. (2004). Volcanism, CO_2 and palaeoclimate: a Late Jurassic–Early Cretaceous carbon and oxygen isotope record. *Journal of the Geological Society, London, 161,* 695–702.

Wilmsen, M., & Nagm, E. (2012). Depositional environments and facies development of the Cenomanian–Turonian Galala and Maghra el Hadida formations of the Southern Galala Plateau (Upper Cretaceous, Eastern Desert, Egypt). *Facies, 58(2),* 229–247.

Wilmsen, M., & Nagm, E. (2013). Sequence stratigraphy of the lower Upper Cretaceous (upper Cenomanian–Turonian) of the Eastern Desert, Egypt. *Newsletters on Stratigraphy, 46,* 23–46.

Wilmsen, M., Niebuhr, B., Chellouche, P., Pürner, T., & Kling, M. (2010). Facies pattern and sea-level dynamics of the early Late Cretaceous transgression: a case study from the lower Danubian Cretaceous Group (Bavaria, southern Germany). *Facies, 56,* 483–507.